

# Biped Robot Gait Control Based on Enhanced Capture Point

Zhongyuan Tian<sup>1</sup>, Mingguo Zhao<sup>2</sup>

**Abstract**—In this paper, we propose the concept of enhanced capture point. Then we develop the enhanced CP controller with two enhanced CP control methods eCPS, eCPT. Their stability and disturbance rejection ability are analyzed. In addition, we introduce the concept of controllable region of CP and compare the enhanced CP control with CP control on the disturbance rejection performance. The simulation results of the linear inverted pendulum model verify the effectiveness of the proposed method, and the use of eCPT to achieve a more stable gait of the robot.

## I. INTRODUCTION

It has been more than 50 years since the world's first bipedal robot was built by Kato et al. at the University of Tokyo in 1967[1],[2]. But the development of biped robots is still slow. The challenge is to improve the stability and robustness of biped walking, especially when in the presence of external disturbances. Vukobratovic and Stepanenko et al. [3], [4] proposed the concept of Zero Moment Point (ZMP), which provides guidelines for the balance control of biped robots. Later, many scholars proposed some gait planning methods and balance control methods based on ZMP.

Kajita proposed a linear inverted pendulum model [5]. According to its dynamics, the position and velocity of the center of mass (CoM) can be calculated if we know the position of the support point, so the gait generation can be realized easily. In order to smooth the speed of CoM while step changes, kajita further proposed a cart-table model [6], [7]. By using the model predictive control on the cart-table model, stable CoM pattern is generated according to the prescribed ZMP trajectory.

Jerry Pratt [8] proposed capture point (CP) based on LIPM. CP is the divergent component of the LIPM dynamics. It is the point on the floor onto which the robot has to step to come to a complete rest. Hof also proposed a similar concept: Extrapolated Center of Mass [9].

Englberger et al. proposed two CP control methods, CP end-of-step control (CPS) and CP tracking control (CPT) [10]. When CoM is disturbed, the outer loop CP controller adjust the ZMP in real time to make sure that CP can reach the target CP, and the measured ZMP converges to the adjusted ZMP through the inner loop ZMP control. Later he proposed to preview next three steps for CP reference [11], perfecting the CP-based gait planning method.

\*This work was supported by UBTECH Robotics, Inc..

<sup>1</sup>Department of Automation, Tsinghua University, Beijing 100084, China.  
Email : [ustbkey@163.com](mailto:ustbkey@163.com)

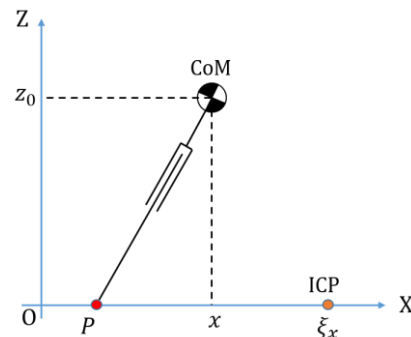


Figure 1. LIPM and Instantaneous Capture Point

In 2009, Takenaka et al. proposed divergent component of motion (DCM) [12]. Later, Englberger et al. extended DCM to 3D and realized the control of the vertical direction of CoM [13]. In 2015, they applied the continuous double support (CDS) and heel-to-toe to the original gait planning [14], so that ZMP becomes continuous and the robot could step further.

However, the proposed CP control methods (CPS and CPT) don't have a good performance on large external disturbance. In order to improve the disturbance rejection ability of the system, we propose the concept of enhanced capture point (eCP) and derive the enhanced CP controller by using eCP.

The paper is organized as follows: section II derives LIPM, CP and two CP control methods: CPS and CPT. Section III introduces an enhanced CP controller and its two enhanced CP control methods: enhanced CPS (eCPS) and enhanced CPT (eCPT). And by introducing the concept of CP controllable region, the advantages and disadvantages of the two controllers are compared. Section IV is the simulation and experimental result, which proves that the enhanced CP controller has better stability. Section V summarizes the full paper.

## II. LIP BASED CP DYNAMICS AND CP CONTROL METHOD

### A. LIP Model

To facilitate modeling and gait planning for robots, Kajita proposed LIPM. The model consists of a particle of mass  $M$  and a massless telescopic leg. Its 2D map in sagittal plane is shown in Fig. 1. The analysis in frontal plane is similar with

<sup>2</sup>Center for Brain-Inspired Computing Research (CBICR), Beijing Innovation Center for Future Chip, Optical Memory National Engineering Research Center, & Department of Automation, Tsinghua University, Beijing 100084, China. Email : [mgzhao@mail.tsinghua.edu.cn](mailto:mgzhao@mail.tsinghua.edu.cn)

sagittal plane. The height of CoM is  $z_0$  and the support point is  $P$ . We can get its dynamic expression by analyzing the force of the LIPM as

$$\ddot{\mathbf{x}} = \frac{g}{z_0}(\mathbf{x} - \mathbf{p}), \quad (1)$$

also the analytical expression of CoM position and velocity :

$$\mathbf{x}(t) = (\mathbf{x}_i - \mathbf{p}) \cosh(\omega t) + \frac{\dot{\mathbf{x}}_i \sinh(\omega t)}{\omega} + \mathbf{p}, \quad (2)$$

$$\dot{\mathbf{x}}(t) = \omega(\mathbf{x}_i - \mathbf{p}) \sinh(\omega t) + \dot{\mathbf{x}}_i \cosh(\omega t). \quad (3)$$

$\mathbf{x}_i, \dot{\mathbf{x}}_i$  are the initial position and velocity of CoM respectively, and  $\omega = \sqrt{g/z_0}$ . We will find that CoM acceleration and position of the LIPM are linear. In the gait planning, the CoM state at any time can be calculated by giving an appropriate initial value of CoM position, velocity and the support point. Therefore, the introduction of LIPM greatly facilitates gait planning.

### B. CP Dynamics

Jerry Pratt proposed the concept of capture point based on LIPM:

$$\xi = \mathbf{x} + \frac{\dot{\mathbf{x}}}{\omega}. \quad (4)$$

$\xi$  is a linear combination of  $\mathbf{x}$  and  $\dot{\mathbf{x}}$ . As shown in Fig. 1,  $\xi_x$  is the instantaneous capture point (ICP). We choose  $\mathbf{x}, \xi$  as the state variable, and (1) can be reduced to two first-order equations:

$$\dot{\mathbf{x}} = -\omega(\mathbf{x} - \xi), \quad (5)$$

$$\dot{\xi} = \omega(\xi - \mathbf{p}). \quad (6)$$

(5) shows that the stable component  $\mathbf{x}$  eventually converges to  $\xi$ , the direction of  $\mathbf{x}$  always points to  $\xi$ , and (6) indicates that the divergent component  $\xi$  is gradually away from ZMP. Therefore, we only need to control  $\xi$  to the target position, and  $\mathbf{x}$  will automatically converge to  $\xi$ .

### C. CP Control Methods

The time domain expression of  $\xi$  can be obtained by integrating equation (6):

$$\xi(t) = \mathbf{p} + e^{\omega t}(\xi_0 - \mathbf{p}). \quad (7)$$

Assume that  $\xi$  and  $\xi_0$  are target CP and ICP respectively, and replace  $\xi_0, \xi, t$  with  $\xi, \xi_{des}, dT$ , we can derive the control law of CP:

$$\mathbf{p} = \frac{\xi_{des} - e^{\omega dT} \xi}{1 - e^{\omega dT}}. \quad (8)$$

The stability and robustness of the CP control law (8) is validated in [10]. Engelsberger et al. proposed two CP control methods according to (8).

#### 1) CP end-of-step Control (CPS)

As shown in Fig. 2,  $\xi$  is ICP,  $\xi_{des}$  is the target position that  $\xi$  will reach at the end of current step.  $\xi_{des} = \xi_i, i = 1, 2, 3 \dots$ . The black solid line is the reference trajectory of  $\xi$ .  $\xi$  will move from the previous pink point to the next one.  $dT$  is

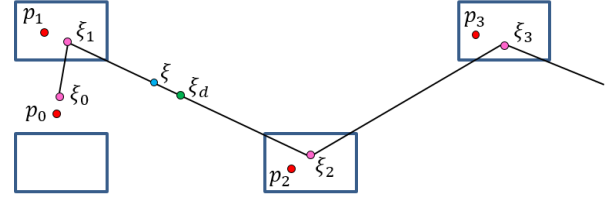


Figure 2. Two-dimensional CP shifting mechanism

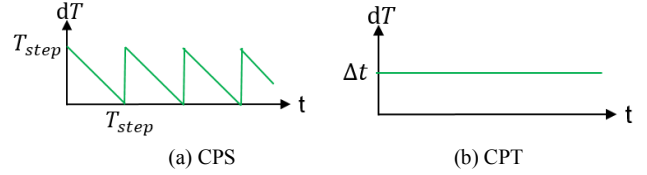


Figure 3. Generation of dT patterns

shown by the green line in Fig. 3(a), and its slope is -1. We can see that  $\xi_{des}$  is a constant and  $dT$  is a decreasing variable. The control goal of CPS is to adjust ZMP so that  $\xi$  can reach  $\xi_{des}$  at the end of a gait period.

#### 2) CP Tracking Control (CPT)

In this method,  $\xi_{des}$  is the target value that  $\xi$  will arrive after  $dT$ .  $\xi_{des} = \xi_d$ . Unlike CPS,  $\xi_{des}$  is an increasing variable and  $dT$  is a constant, as shown in Fig. 3(b). The control goal of CPT is to adjust ZMP so that  $\xi$  can track the trajectory of  $\xi_{des}$ .

#### 3) Projection Criteria of Desired ZMP

We must try to ensure that ZMP is inside the support polygon in gait planning. If the desired ZMP is outside the support polygon in CP control, we need to change ZMP to a place closest to it. This may cause that  $\xi$  fail to reach the target position accurately at current step, but it will be corrected in the next step. Please refer to [10] for more details about the projection criteria.

#### 4) Position Based ZMP Control

ZMP control is needed if there is a deviation between the desired ZMP and the measured ZMP. This can be caused by uneven road, errors in multi-body model and LIPM et al. We use a position based ZMP control proposed in [15]. The ZMP control law is

$$\ddot{\mathbf{x}}_d = k_f F_z / z_c (\mathbf{p}_x - \mathbf{p}_{x,d}). \quad (9)$$

This is a proportional feedback controller.  $k_f$  is the proportional gain and  $F_z / z_c$  is a constant.  $\mathbf{x}_d$  and  $\dot{\mathbf{x}}_d$  can be obtained by integration.

## III. ENHANCED CP CONTROL

The criterion for judging that robot can walk stably is ZMP is inside the supporting polygon. So we will try to keep ZMP close to the center of the support polygon, which will enhance the stability of the system. For CPS, if CoM is disturbed, ICP will deviate from the planned position. Then ZMP is adjusted by the controller (8) so that ICP can still reach the target CP.

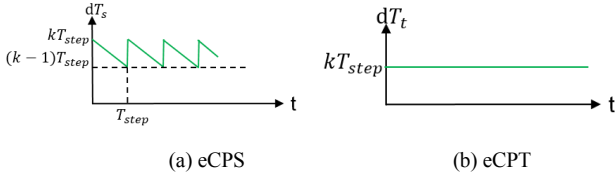


Figure 4. Generation of  $dT_s, dT_t$

However, when ICP close to  $\xi_{des}$ , a small disturbance will cause the desired ZMP to deviate far from the support polygon. That is, the disturbance rejection performance of the CPS is gradually declined in a gait period. For CPT, since the distance between ICP and  $\xi_d$  is relatively close, even a small disturbance can easily make ZMP out of the range of support polygon, so the disturbance rejection ability of CPT is weaker than CPS.

In order to enhance the disturbance rejection ability of the system, this paper proposes an enhanced CP based on (7):

$$\xi_e(T) = \mathbf{p} + e^{\omega T}(\xi - \mathbf{p}), \quad (10)$$

$T > T_{step}$ . The enhanced CP refers to the point at which the ICP arrives after more than one gait period. We derive two enhanced CP control methods by using (10).

#### A. Enhanced CP end-of-step Control

We can derive the enhanced CPS control law by replacing  $\xi_e, T$ , with  $\xi_{e,s}, dT_s$

$$\mathbf{p} = \frac{\xi_{e,s} - e^{\omega dT_s} \xi}{1 - e^{\omega dT_s}}. \quad (11)$$

In order to make gait planning more convenient, we take  $dT$  as an integer multiple of the period.

$$\xi_{e,s} = \mathbf{p} + e^{\omega k T_{step}}(\xi_0 - \mathbf{p}), \quad (12)$$

$k > 1$ .  $dT_s$  is shown by the green line in Fig. 4(a). (11) can be written as

$$\mathbf{p} = \frac{\xi_{e,s} - \xi + \xi - e^{\omega dT_s} \xi}{1 - e^{\omega dT_s}}, \quad (13)$$

$$\mathbf{p} = \frac{\xi_{e,s} - \xi}{1 - e^{\omega dT_s}} + \xi. \quad (14)$$

According to gait parameters used in our robot, let  $\mathbf{p}=0.25\text{m}$ ,  $\xi=0.2569\text{m}$ , when  $k=2, 3, 4$ ,  $\xi_{e,s}$  and  $\xi_{e,s}/\xi$  are shown in TABLE I. It can be seen that when  $k \geq 3$ ,  $\xi_{e,s}/\xi > 10^3$ ,  $\xi_{e,s} \gg \xi$ ,  $e^{\omega dT_s} \gg 1$ . Therefore, (14) can be further reduced to

$$\mathbf{p} = \xi - \frac{\xi_{e,s}}{e^{\omega dT_s}}. \quad (15)$$

TABLE I. THE VALUE OF  $\xi_{e,s}, \xi_{e,s}/\xi$  WITH DIFFERENT K

	k=2	k=3	k=4
$\xi_{e,s}(m)$	9.8	353.8	1313.4
$\xi_{e,s}/\xi$	38	1377	5112

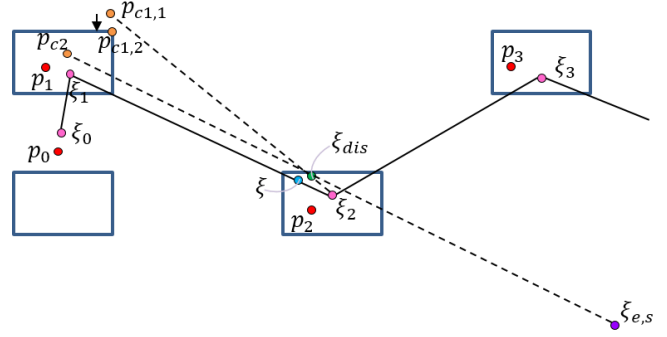


Figure 5. shifting mechanism with eCPS

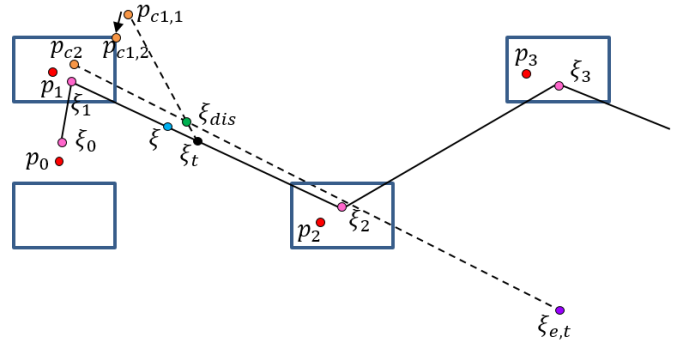


Figure 6. shifting mechanism with eCPT

(15) is the final eCPS control law and  $\xi_{e,s}$  can be calculated by

$$\xi_{e,s} = \mathbf{p} + e^{\omega k T_{step}}(\xi_0 - \mathbf{p}), \quad k \geq 3. \quad (16)$$

The eCPS and CPS are identical if there is no disturbance. However, when CoM is disturbed, eCPS reduces the adjustment of the desired ZMP by selecting a farther CP target ( $\xi_{e,s}$ ).

As shown in Fig. 5, the pink dots represent desired position of  $\xi$  for every step, and the red dots are reference ZMP. The blue dot represents ICP at a certain moment, and the green dot represents disturbed ICP which is deviated from the planned trajectory. According to CPS, the adjusted ZMP  $\mathbf{p}_{c1,1}$  is beyond the footprint area. We select the closest point on the edge of the footprint  $\mathbf{p}_{c1,2}$  as the adjusted ZMP according to the projection criterion. We will find that  $\xi$  cannot reach  $\xi_i$

at the end of current step, and robot falls easily because the adjusted ZMP is on the edge of the support polygon.

The purple dots in Fig. 5 represent enhanced CP. It is easy to know that the adjusted ZMP  $\mathbf{p}_{c2}$  calculated by eCPS is closer to the footprint center than CPS according to the geometric relationship. This shows eCPS has better disturbance rejection ability.  $\xi$  will reach a point near  $\xi_i$  at the end of current gait period, and it can reach  $\xi_{i+1}$  at the next step.

#### B. Enhanced CP Tracking Control

We can derive the enhanced CPT control law from (10)

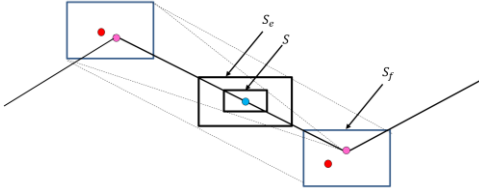


Figure 7. Controllable region of CP control and eCP control

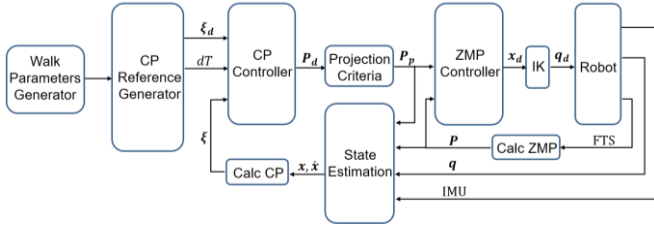


Figure 8. Overall control block diagram

by replacing  $\xi_e, T$  with  $\xi_{e,t}, dT_t$

$$\mathbf{p} = \frac{\xi_{e,t} - e^{-\omega dT_t} \xi}{1 - e^{-\omega dT_t}}. \quad (17)$$

$\xi_{e,t}$  is the tracking target of  $\xi$  which is planned in advance

$$\xi_{e,t}(t) = \mathbf{p} + e^{\omega(kT_{step}+t)}(\xi_0 - \mathbf{p}). \quad (18)$$

$dT_t$  is a constant as shown in Fig. 4(b). The same as eCPS, when  $k \geq 3$ ,  $\xi_{e,t}/\xi > 10^3$ ,  $\xi_{e,t} \gg \xi$ ,  $e^{\omega T_t} \gg 1$ , (17) can be further reduced to

$$\mathbf{p} = \xi - \frac{\xi_{e,t}}{e^{\omega dT_t}}. \quad (19)$$

(19) is the final eCPS control law and  $\xi_{e,t}$  can be calculated by

$$\xi_{e,t}(t) = \mathbf{p} + e^{\omega(kT_{step}+t)}(\xi_0 - \mathbf{p}), \quad k \geq 3. \quad (20)$$

The improvement of eCPT is that it increases the distance between ICP and the tracking target, which reduces the sensitivity to disturbances.

In Fig. 6 the blue dot indicates ICP, and the green dot represents disturbed ICP. The adjusted ZMP  $\mathbf{p}_{c1,1}$  calculated according to CPT is beyond the footprint area. The selected point  $\mathbf{p}_{c1,2}$  is on the edge of the support polygon. This can cause instability when walking. However, since  $\xi_{e,s}$  is far from  $\xi$ , the adjusted  $\mathbf{p}_{c2}$  is closer to the footprint center than CPT, so it is easy to see that eCPT has better disturbance rejection ability than CPT.

### C. Controllable Region of CP

In order to compare the disturbance rejection performance of CPS and eCPS, the controllable region of CP is proposed [16]. The blue dot in Fig. 7 indicates ICP. The greater the disturbance to CoM, the further the distance CP deviates from the planned position. The adjusted ZMP will be within the footprint area as long as the disturbed ICP stay in S. We call S as controllable region of CP. The controllable region

of enhanced CP  $S_e$  can be calculated in the same way.  $S_f$  represents the footprint area.

It is easy to know that S is reduced from  $S_f$  to 0, and  $S_e$  always maintains the maximum value  $S_f$ . So we can see that enhanced CP control has better disturbance rejection performance from the performance index of the controllable region.

### D. the Advantages of enhanced CP control

The advantages of enhanced CP control are summarized as follows:

- When  $\xi$  is disturbed by external disturbance, the adjusted ZMP obtained by eCP control is closer to the center of the footprint. It has better stability than CP control.
- The controllable region of eCP control always maintains maximum value. Its disturbance rejection performance is better than CP control.

### E. Overall Control Block Diagram

Fig. 8 shows an overview of overall control block diagram. Walk parameters generator and CP reference generator set the gait parameters. The main task of the outer loop is to control ICP to reach the target CP. While the task of inner loop is to reduce the error of measured ZMP with desired ZMP. The data of IMU, ZMP and joint angle are used to calculate the current state of CoM.

## IV. SIMULATIONS AND EXPERIMENTS

We apply eCP control algorithm to the single particle model in simulink and our robot. The superiority and practicality of eCP Control law has been verified.

### A. Simulations

In this paper, a 3D-LIP model is established in simulink. Its mass of CoM is 40kg, the height of CoM is 0.8m from the ground, the gait period is 0.8s, and the foot width is 0.14m. The foot length is 0.19m, the step length of each step is 0.3m, and the step width is 0.2m. Perform the same task using CPS and eCPS respectively: move forward 6 steps and come to a stop. The simulation block diagram is similar with robot control block diagram. The differences is that robot is replaced by LIPM. The ICP is calculated by the linear inverted pendulum dynamics, and the external force disturbance is added to the centroid.

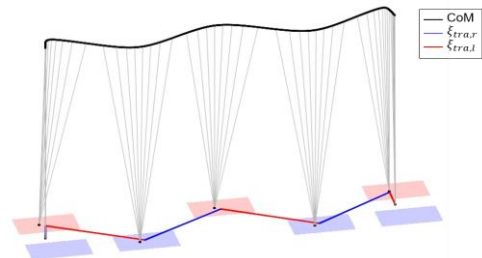


Figure 9. Simulation results without disturbance from 3D view

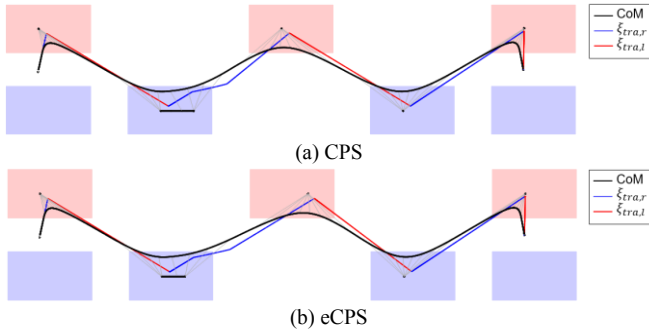


Figure 10. Simulation results with small disturbance

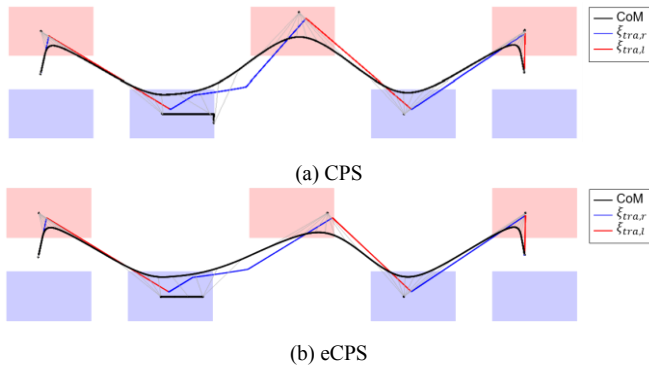


Figure 11. Simulation results with medium disturbance

Fig. 9 is the result without external force disturbance from 3D view. The black line represents CoM trajectory, the blue lines and the red lines are CP trajectory during right and left foot support, the black points are ZMP and the gray lines represent pendulums.

In order to test the disturbance rejection performance of the two control law, we add 0.2s external force disturbance in the x direction in SSP of the third step. Both of CPS and eCPS can resist the interference when the external force is small, as shown in Fig. 10, ICP can reach the target CP at the end of third step.

When the interference force is 180N, the adjusted ZMP obtained according to CPS exceeds the footprint area, and the closest point on the front edge of the footprint is selected as the adjusted ZMP by the projection criterion. As shown in Fig. 11(a), ICP deviates from the target CP at the end of the third step, and reaches the target CP at the fourth. In Fig. 11(b), for the same interference, the adjusted ZMP obtained by eCPS is always in the range of the footprint area. It shows better disturbance rejection performance of eCPS.

When the external force reaches 200N, as shown in Fig. 12(a), the ICP is diverged in the fourth step with CPS. For eCPS, as shown in Fig. 12(b), the adjusted ZMP of the third step stays within the footprint area, and ICP reaches target CP at the end of the fourth step. Therefore, it can be seen eCPS has greater disturbance rejection ability than CPS.

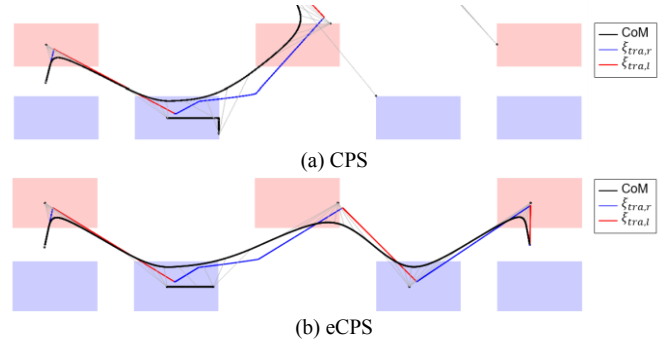


Figure 12. Simulation results with big disturbance

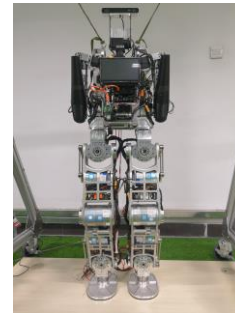


Figure 13. Walker

## B. Experimental Results

As shown in Fig. 13, the robot “walker” has 12 DOFs, weighs about 46kg, height is 1.35m, leg length is 0.7m, foot length is 22.75cm, foot width is 17cm, and the control period is 1 ms.

Since CPS has poor disturbance rejection performance at the end of a gait period, two methods of CPT and eCPT are compared in the robot experiment. We use open-loop gait in X direction and CPT, eCPT in Y direction. The robot moves forward six steps in a straight line and comes to a stop. The experiment was carried out on the lawn because it can provide greater external disturbances than flat ground. The gait period is 1.2s, DSP is 0.36s, the step size is 0.25m, the step width is 0.205m, the height of the hip joint is 0.77m, the height of CoM is about 0.6m, and dT are 0.05T<sub>step</sub> and 3T<sub>step</sub>, respectively.

Fig. 14 and Fig. 15 record CoM, CP and ZMP data of the two methods in Y direction respectively. There is a small deviation between the planned and measured positions of CoM in both figures. The planned and measured CP have large deviations at the beginning of each step, and then gradually decrease, which is caused by the collision when swinging foot lands. However, the deviation of eCPT is greater than CPT, because the target CP of eCPT is farther, and its tracking trajectory is different from CPT.

The adjusted ZMP has a large variation and its oscillation is obvious in Fig. 14 while the variation is small in Fig. 15. The measured ZMP in Fig. 15 is more moderate than ZMP in Fig. 14. This shows the advantage of eCPT that

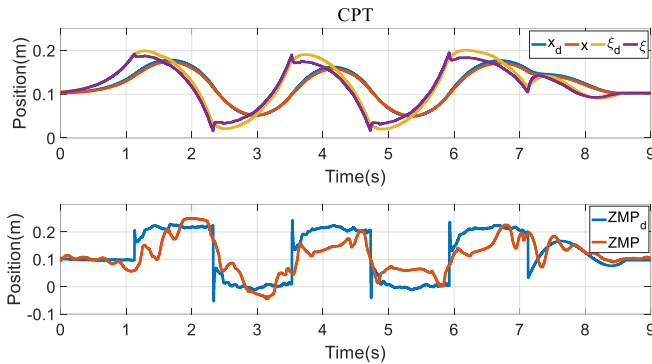


Figure 14. Experimental results of CPT

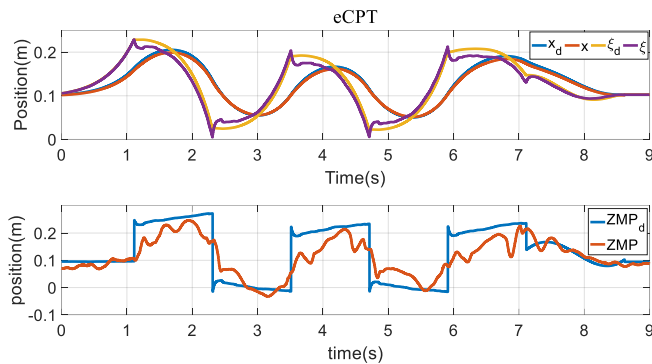


Figure 15. Experimental results of eCPT

selecting a farther target CP and its better stability. The disturbance rejection ability of eCP Control in Y direction has been proven to be good, and we will apply it in both X and Y directions in our future work.

## V. SUMMARY AND FUTURE WORK

The main contribution of this article is that we define enhanced capture point (eCP). It is the point that capture point will arrive after more than one step period. By choosing eCP as the target CP in CP control, we develop the enhanced CP controller with two enhanced CP control methods eCPS, eCPT. Their controllable region of CP keeps maximum throughout gait period, which is much better than CP control. So the new methods can resist greater external interference. In addition, eCP control has a smaller adjustment on ZMP than CP control as for the same external force which means eCP control have better stability while walking. The performance of eCP control is validated in Simulink and our robot can walk stably on the lawn by using it. Our future work includes :

- Apply enhanced CP control to realize omnidirectional gait.
- Develop the method of foot landing control and online planning of swing foot.

## ACKNOWLEDGMENT

The authors would like to thank the UBTECH's staff from Beijing Research Institute for providing the humanoid robot WALKER, also thank Haitao Wang, Rongge Zhang, Qilun Wang, Xueheng Zhang and Wenbin Hu for their constructive suggestions.

## REFERENCES

- [1] M. Akhtaruzzaman and A. A. Shafie, "Evolution of Humanoid Robot and contribution of various countries in advancing the research and development of the platform," ICCAS 2010, Gyeonggi-do, 2010, pp. 1021-1028.
- [2] Lim H, Takanishi A. Biped walking robots created at Waseda University: WL and WABIAN family [J]. Philosophical Transactions of the Royal Society of London A: Mathematical, Physical and Engineering Sciences, 2007, 365(1850): 49-64.
- [3] M. Vukobratovic and D. Juricic, "Contribution to the Synthesis of Biped Gait," in IEEE Transactions on Biomedical Engineering, vol. BME-16, no. 1, pp. 1-6, Jan. 1969.
- [4] Vukobratović M, Borovac B. Zero-moment point—thirty five years of its life [J]. International journal of humanoid robotics, 2004, 1(01): 157-173.
- [5] Kajita S, Kanehiro F, Kaneko K, et al. The 3D Linear Inverted Pendulum Mode: A simple modeling for a biped walking pattern generation[C]//Intelligent Robots and Systems, 2001. Proceedings. 2001 IEEE/RSJ International Conference on. IEEE, 2001, 1: 239-246.
- [6] Kajita S, Kanehiro F, Kaneko K, et al. Biped walking pattern generation by using preview control of zero-moment point[C]//Robotics and Automation, 2003. Proceedings. ICRA'03. IEEE International Conference on. IEEE, 2003, 2: 1620-1626.
- [7] Kajita S, Hirukawa H, Harada K, et al. Introduction to humanoid robotics [M]. Springer Berlin Heidelberg, 2014.
- [8] Pratt J, Carff J, Drakunov S, et al. Capture point: A step toward humanoid push recovery[C]//Humanoid Robots, 2006 6th IEEE-RAS International Conference on. IEEE, 2006: 200-207.
- [9] Hof A L. The 'extrapolated center of mass' concept suggests a simple control of balance in walking [J]. Human movement science, 2008, 27(1): 112-125.
- [10] Engelsberger J, Ott C, Roa M A, et al. Bipedal walking control based on capture point dynamics[C]//Intelligent Robots and Systems (IROS), 2011 IEEE/RSJ International Conference on. IEEE, 2011: 4420-4427.
- [11] Engelsberger J, Ott C. Integration of vertical com motion and angular momentum in an extended capture point tracking controller for bipedal walking[C]//Humanoid Robots (Humanoids), 2012 12th IEEE-RAS International Conference on. IEEE, 2012: 183-189.
- [12] Takenaka T, Matsumoto T, Yoshiike T. Real time motion generation and control for biped robot-1 st report: Walking gait pattern generation[C]//Intelligent Robots and Systems, 2009. IROS 2009. IEEE/RSJ International Conference on. IEEE, 2009: 1084-1091.
- [13] J. Engelsberger, C. Ott and A. Albu-Schäffer, "Three-dimensional bipedal walking control using Divergent Component of Motion," 2013 IEEE/RSJ International Conference on Intelligent Robots and Systems, Tokyo, 2013, pp. 2600-2607.
- [14] Engelsberger J, Ott C, Albu-Schäffer A. Three-dimensional bipedal walking control based on divergent component of motion [J]. IEEE Transactions on Robotics, 2015, 31(2): 355-368.
- [15] Slotine J J E, Li W. On the adaptive control of robot manipulators [J]. The international journal of robotics research, 1987, 6(3): 49-59.
- [16] Kang Y, Tian Z, Zhao M. The ICP-based controllability criterion and its application to bipedal walking control[C]//Robotics and Biomimetics (ROBIO), 2017 IEEE International Conference on. IEEE, 2017: 2425-2432.